Earth Surface Processes and Landforms
Earth Surf. Process. Landforms **23**, 509–525 (1998)

FRACTAL INTERRELATIONSHIPS BETWEEN TOPOGRAPHY AND STRUCTURE

THOMAS H. WILSON* AND JOVITA DOMINIC
Department of Geology and Geography, West Virginia University, Morgantown, WV 26506, USA

Received 23 September 1996; Revised 21 June 1997; Accepted 15 September 1997

ABSTRACT

Fractal interrelationships between topography and structure are investigated in two areas of the North American central Appalachian Mountains: one in the intensely deformed Valley and Ridge province and the other in the relatively undeformed foreland area of the Appalachian Plateau province.

In the Valley and Ridge province the fractal dimensions of topographic and structural relief vary systematically along the strike of major folds following a second-order polynominal trend. Cross-correlation of the fractal dimensions of topography to structure indicates that there is a significant positive correlation between the two. Fractal analysis of topography in the relatively undeformed foreland area of the Appalachian Plateau revealed no significant variation in the fractal characteristics of topography across the study area, consistent with the lack of near-surface structure. However, fractal analysis of deeper structures beneath the Plateau area undertaken using reflection seismic data revealed step-wise increases in fractal dimension from the deeply buried Precambrian basement to the near-surface. These vertical changes in fractal dimension can be related to the tectonic history of the area.

Taken together, these studies indicate that fractal analysis provides a means to quantify and compare the influence of near-surface structure on topographic development and lateral and vertical structural variability. Fractal analysis provides a means to characterize the systematic changes in the complex patterns formed by topography and structure and the interrelationships between them. Similarity in their fractal characteristics implies similarity in the relative amplitude and abundance of different wavelength features in the topographic or structural profile. © 1998 John Wiley & Sons, Ltd.

KEY WORDS: fractal; fractal interrelationships; fractal dimension; topography; structure; spatial distribution

INTRODUCTION

The purpose of this paper is to demonstrate that fractal analysis reveals systematic changes in the appearance of topography and near-surface structure and can be used to quantify systematic interrelationships between them. The study incorporates fractal analysis of topography, structural cross-sections and reflection seismic data.

Fractal analysis of topography presented in the literature yields a variety of different results. For example, power spectral analysis of 30 m digital elevation models (DEMs) and Sea Beam centre-beam depths (Gilbert, 1989) often contain non-linear regions in log–log plots of power spectra which imply non-fractal behaviour outside a certain range. Gilbert also notes that different results can be obtained depending upon how the data are decimated or interpolated. Mareschal (1989) uses a fractal model to optimize the reconstruction of sea-floor topography from limited data. Mark and Aronson (1984) derive estimates of fractal dimension over the range of scales present in numerous 7½ min quadrangles and note the presence of multiple fractal regions, one below 0·6 km and another between 0·6 and 5 km. At scales above 5 km their results suggest the fractal model breaks down. Goodchild (1980) makes similar observations concerning the fractal dimensions of coastlines. Whereas Mandelbrot (1967, 1977) generally assumes scale invariance, Goodchild (1980) rewalked the east coast of Britain and found two linear regions with fractal dimensions (D) of 1·31 (larger scale) and 1·15 (detail features). Goodchild's discussion of Hakansan's (1978) work suggests that scale-variance observed in the data could be related to the technique employed to estimate D and to the degree of cartographic generalization in maps drawn at different scales. Klinkenberg and Goodchild (1992) examine the fractal properties of topography in 55 DEMs

* Correspondence to: T. H. Wilson, Department of Geology and Geography, West Virginia University, Morgantown, WV 26506, USA.

CCC 0197-9337/98/060509–17 $17.50

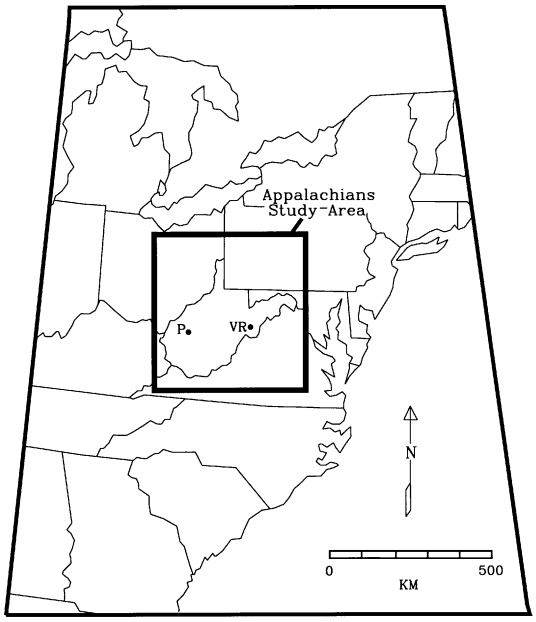

Figure 1. Location of the Appalachians study area in eastern North America

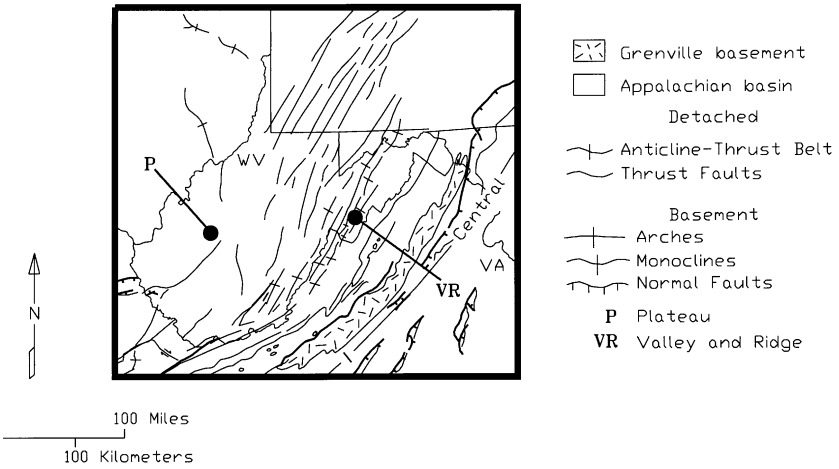

Figure 2. Locations of the Valley and Ridge (VR) and Plateau (P) areas of the central Appalachian Mountains

from seven different physiographic provinces. They find the fractal model is applicable in most, but not all, cases. Some studies suggest that the fractal dimension of topography does not vary from one tectonic province to another (e.g. Turcotte, 1992), while other studies imply that significant variation is present (e.g. Mark and Aronson, 1984; Klinkenberg and Goodchild, 1992).

Tectonic processes are generally considered to have fractal properties in both time and space. Active tectonic processes represented by earthquake activity are also shown to represent a fractal process through the Gutenberg–Richter frequency–magnitude relationship which is equivalent to a fractal interrelationship between the frequency of earthquake occurrence and the characteristic linear dimension of the fault plane (Aki, 1980; Turcotte, 1989; Rundle, 1989). Surface fracture traces (Barton and Hsieh, 1989; Walsh and Watterson, 1993) and active faults (Hirata, 1989) form fractal patterns, and fractal models of fault systems accurately predict the relative velocities of fault motion along main and higher-order fault strands (Turcotte, 1986). Fragment size (Turcotte, 1986) and fold wavelength (Wu, 1993; Wilson, 1997) also have fractal distributions. In

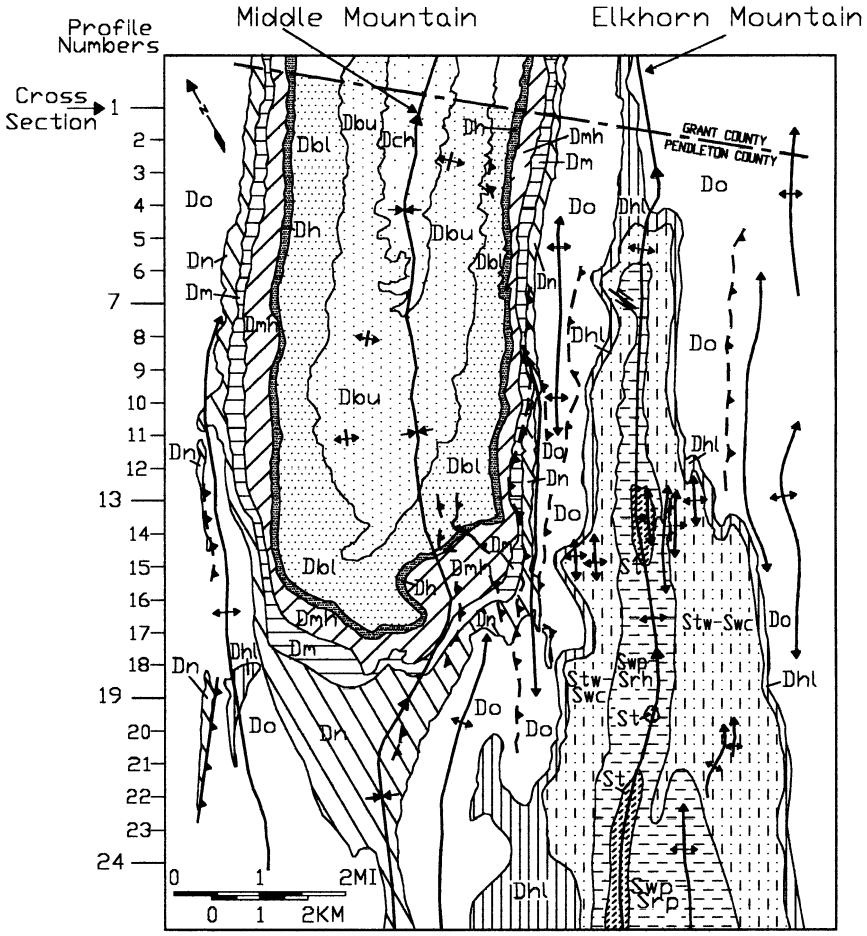

Figure 3. Detailed geological map of the Valley and Ridge study area. Stratigraphic intervals exposed in the area extend from the Lower Silurian Tuscarora sandstone (St) to the Upper Devonian Chemung Formation (Dch)

general, previous studies indicate that both extension and compression tectonic processes take place through a fractal distribution of strain. In the following studies, the fractal characteristics of topography are evaluated within the context of associated structure in two areas of the central Appalachian mountains in eastern North America (Figures 1 and 2).

The first study (VR in Figures 1 and 2) was conducted in the Valley and Ridge province of the central Appalachians. This area represents a case where near-surface deformation is significant and easily recognized in the topography. Significant plunge and variation in the intensity of both folds and faults occur along the major structures of this area.

The second study (P in Figures 1 and 2) was conducted in the relatively undeformed foreland of the Appalachian Plateau province of eastern North America. This example represents a limiting case where topography is developed in an undeformed and unfaulted blanket of sediments. The area overlies the east margin of an ancient aulacogen known as the Rome Trough. Development of the aulacogen occurred primarily during the Middle and Late Cambrian; however, minor recurrent movement including structural inversion is observed throughout the Palaeozoic (Wilson *et al*., 1994). Faults associated with the aulacogen originate in the Precambrian basement and do not extend to the surface. Analysis of this area includes examination of the fractal characteristics of subsurface structures observed in reflection seismic data.

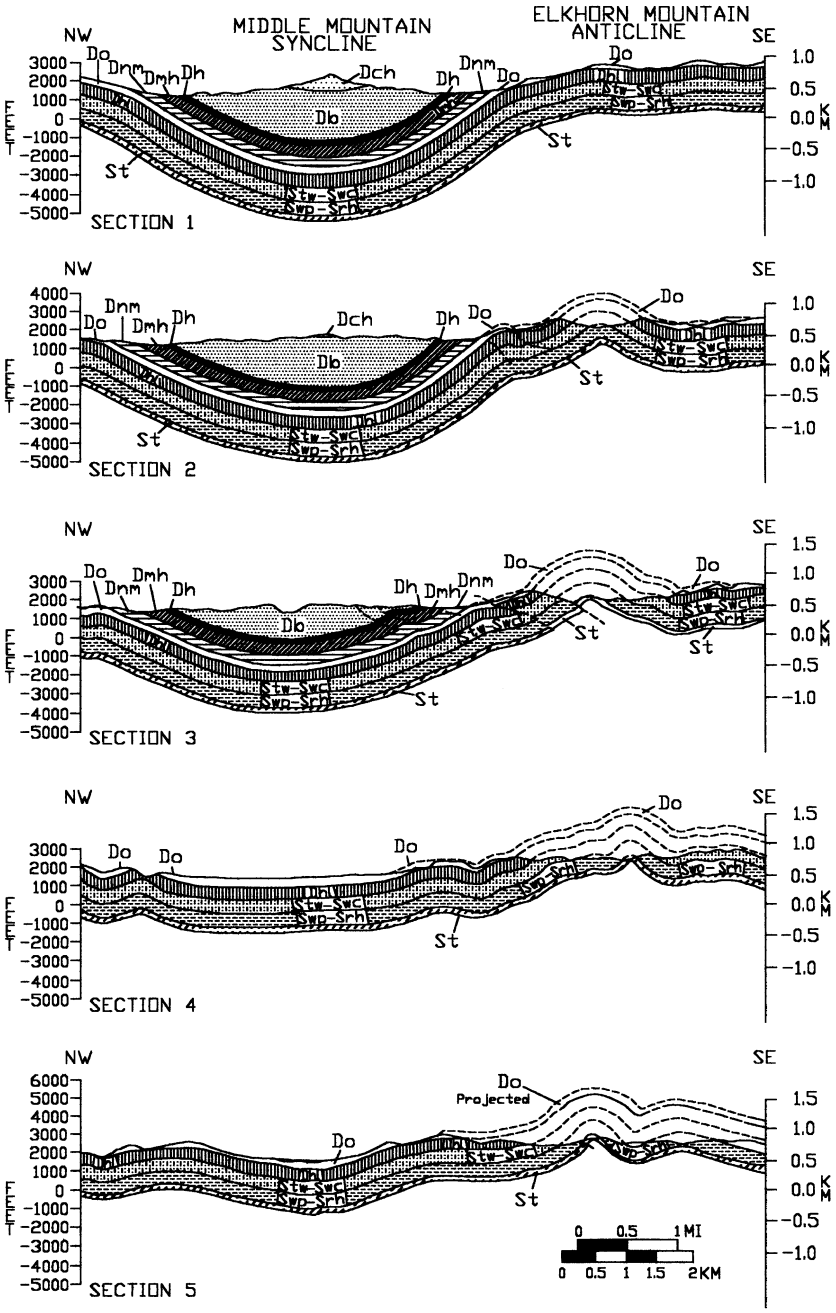

Figure 4. Structural cross-sections constructed northeast-to-southwest through the area lie along topographic profiles 1, 7, 13, 19 and 24 (Figure 3)

APPALACHIAN VALLEY AND RIDGE

Structural setting

The Valley and Ridge province of the central Appalachians is intensely folded and faulted by detached structures formed during the late Palaeozoic Allegheny orogeny (Figure 2). This orogenic event occurred during the collision of Gondwana and Laurentia, which combined to form the supercontinent of Pangaea. The

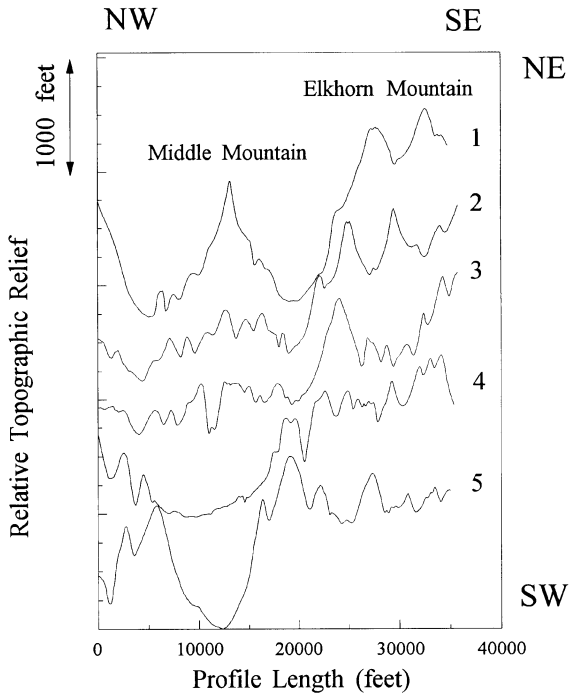

Figure 5. Topographic relief digitized from 7½ minute USGS quadrangles along structural cross-sections 1 to 5 (Figure 4)

near-surface structures of the Valley and Ridge were carried aloft large blind thrust sheets along which as much as 50 per cent shortening occurred (Wilson and Shumaker, 1988, 1992). Near-surface Silurian and Devonian intervals exposed in the study area form an anticline/syncline pair (Figure 3). A series of cross-sections along the Middle Mountain syncline and Elkhorn Mountain anticline (Figure 4) reveal significant differences in relief and relative abundance of different order folds. Structural relief along the Devonian Oriskany Sandstone (Do) on Section 1, for example, is nearly 2 km, and shortening is accommodated primarily by the long wavelength Middle Mountain/Elkhorn Mountain structure. To the southwest, shortening is accommodated by shorter wavelength folds, and structural relief across the first-order Middle Mountain/Elkhorn Mountain fold pair falls to approximately 1·2 km.

The fractal characteristics of topography were evaluated using 24 profiles spaced at approximately 600 m intervals northeast to southwest through the area (see profile numbers in Figure 3). Topographic profiles 1, 7, 13, 19 and 24 (Figure 3) coincide with locations of structural cross-sections 1 to 5 (Figure 4). Elevations were digitized at approximately 15 m intervals along profiles which were constructed from US Geological Survey 7½ minute quadrangles (Figure 5).

Methods

Roughness–length (Malinverno 1990) and compass (Mandelbrot 1967) methods were used to compute fractal dimension. The roughness–length measure is based on the following relationship (Turcotte 1989, 1992):

$$\sigma = \tau^{H} \tag{1}$$

between the standard deviation (σ) and length of window (τ) over which σ is computed. H is referred to as the Hurst exponent (Feder 1988) and is related to *D* through the relationship:

$$D = 2 - H \tag{2}$$

(e.g. Turcotte, 1989). σ is computed from the average standard deviation of data in each of the τ-length subdivisions of the profile. Initially, τ equals the length of the profile and is subsequently diminished in size by a

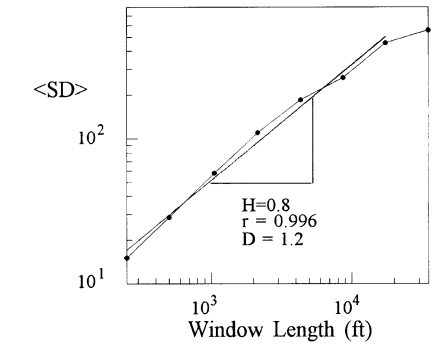

A.

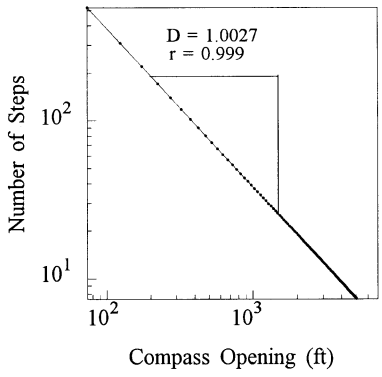

B.

Figure 6. Log–log plots (A) roughness (<SD>) versus window length and (B) number of steps versus compass opening for the roughness–length and compass methods, respectively

factor of 2 at each step. As the window length (τ) decreases, σ is computed from the average standard deviation of the data in 1, and then 2, 4, 8, etc. subdivisions of the profile. Log–log plots of σ are linear if the data have fractal distribution (e.g. Figure 6A) and have slope *H*. In this study the standard deviation associated with the largest window was not included in the computation of *H*. Partial symmetry in the profile causes the standard deviation of the largest window (total profile) to be similar to that of each half of the profile taken separately. This produces the flattening in the slope observed in Figure 6A. Inclusion of the standard deviation of the entire data set into the computation may yield erroneously low *H* (high *D*), hence this value was excluded from all the roughness–length estimates of *D* made in this study.

The compass dimension is derived from the relationship:

$$N = Cr^{-D} \tag{3}$$

Here *N* represents the number of steps taken to traverse the profile, *r* is the compass opening or step length, and *D* is the fractal dimension. Equation 3 is proposed by Mandelbrot (1967) as a modification of Richardson's (1961) observations. Log–log plots of *N* versus *r* are linear with slope $-D$ when *N* has a fractal distribution (e.g. Figure 6B). In this study, estimates of *D* were made from compass openings of 5000 ft and less.

The compass-walking measurements describe the length of the profile measured at different scales, while the roughness–length measurements describe the relative variation of relief at different scales. The compass method measures the self-similar fractal attributes of a profile (e.g. Turcotte 1992). The results of the compass walk vary with arbitrary rescaling of one dimension (e.g. relief or distance along the profile). The roughness–length method measures the self-affine fractal attributes of a profile (e.g. Turcotte 1992). The roughness–length dimension is invariant under arbitrary rescaling of either, or both, profile dimensions.

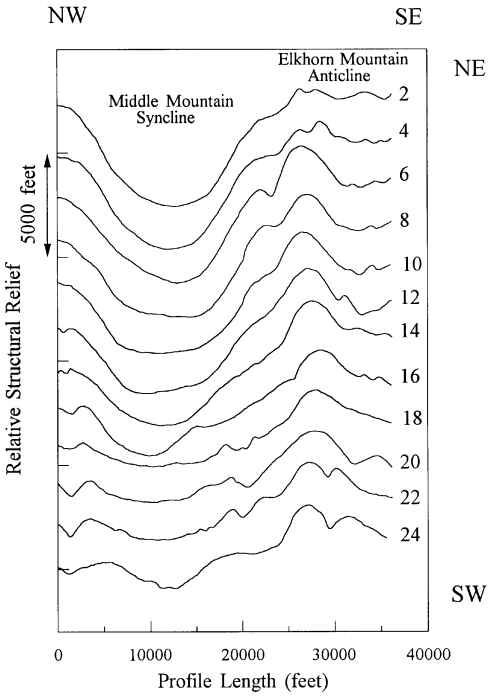

Figure 7. Structural relief of the Oriskany Sandstone compared for the even-numbered cross-sections (see Figure 3) constructed across the Valley and Ridge study area

Results

Interrelationships between topography and near-surface structure are often recognizable. The decrease in structural relief and increased abundance of shorter-wavelength structure observed northeast-to-southwest through the area (see even-numbered profiles, Figure 7) coincide with a decrease in topographic relief and increased abundance of shorter-wavelength topographic features in the landscape (Figure 8). The possibility of interrelationship between these two variables can be assessed simply by evaluating regression line relationships between topographic and structural relief. Correlation coefficients (Figure 9) of regression lines fit to cross-plots of topographic and structural relief along the 24 profiles across the study area were all positive and varied from 0·46 to 0·89. The average value of the correlation coefficients is approximately 0·71. A second-order polynominal fit to the data (Figure 9) has correlation coefficient of 0·57 and suggests increased similarity between structure and topography through the central part of the study area. Just how the topography and structure are related is not implied by the variation of correlation coefficient. Fractals, on the other hand, characterize the relative abundance and amplitude of different wavelength features in a profile. The fractal dimension provides a numerical measure of these attributes in both topographic profiles and structure cross-sections. The extent to which changes in the relative abundance and amplitude of different wavelength folds yields similar changes in the topography can be evaluated by comparing the fractal dimensions of topographic and structural relief.

Roughness–length dimensions computed for each topographic profile rise northeast to southwest through the area (Figure 10A). In the northeastern part of the area there is a steep increase of fractal dimension from approximately 1·18 to 1·35 followed by smaller, irregular increases of D from 1·35 to 1·4 between profiles 8 to 19. In the southwestern end of the area (profiles 20 to 24) fractal dimension drops slightly to an average of approximately 1·35. These variations can be represented by a second-order polynomial (Figure 10A), which has a correlation coefficient (r) of 0·91. Compass dimensions were also computed for each profile (Figure 10B) and are considerably smaller in value than the roughness–length dimensions. Although there is greater variability in the compass dimensions, they form a pattern of variation similar to that observed in the roughness–length

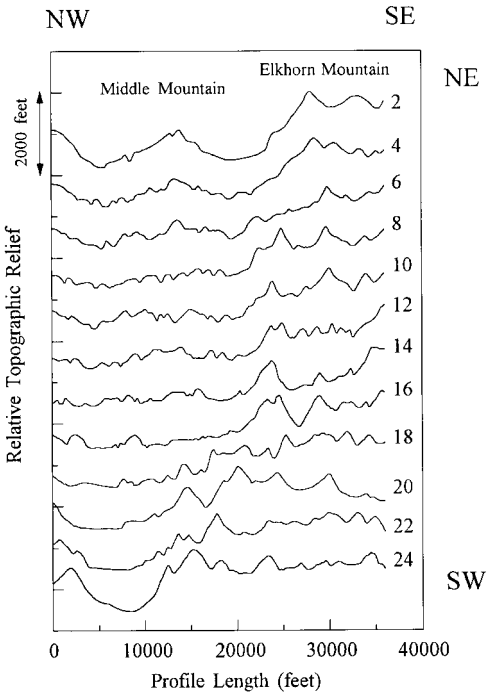

Figure 8. Topographic relief digitized from 7½ minute USGS quadrangles compared for the even-numbered profiles (see Figure 3) across the Valley and Ridge study area

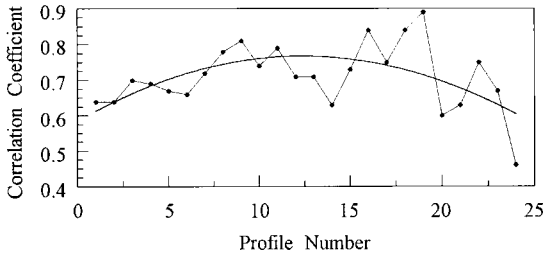

Figure 9. Correlation coefficients between structural and topographic relief plotted for each profile

dimensions and follow a second-order polynomial of similar shape with correlation coefficient $r = 0{\cdot}78$ (Figure 10B). The similarity of the compass and roughness–length measures is suggested in the cross-plots of compass dimension versus roughness–length dimension (Figure 11). The two measures are linearly related to each other with correlation coefficient $r = 0{\cdot}81$.

Similar variation is observed in the fractal dimensions of structural relief along-strike through the area (Figure 12). Second-order polynomials fit to the roughness–length (Figure 12A) and compass dimensions (Figure 12B) have correlation coefficients of 0·89 and 0·6, respectively. The curvilinear trends observed in the fractal dimensions of topography are less apparent. Linear regression lines fit to the roughness–length and compass dimensions yield correlation coefficients (0·85 and 0·6, respectively) similar to those obtained from the second-order polynomial fit.

Topography in the northeastern part of the area is dominated by the Middle and Elkhorn mountains (Figure 8). To the southwest, these mountains are dissected into a series of smaller hills and valleys. The increased roughness of the landscape to the southwest is described by increases of fractal dimension. Increased roughness defined by the roughness–length dimension represents an increase in the amplitude of the shorter-wavelength features relative to the longer-wavelength features in the profile. Structural relief along the Oriskany Sandstone (Figures 4 and 7) is also characterized by an increased abundance of smaller-wavelength folds, northeast to the

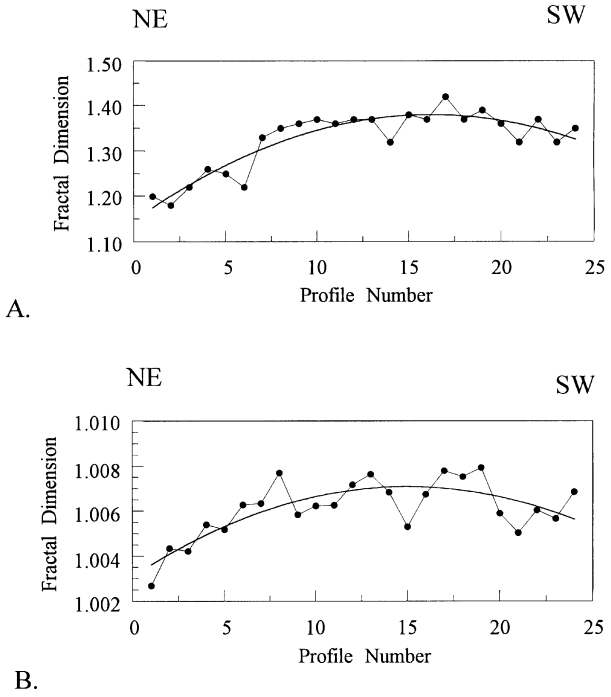

Figure 10. Fractal dimensions obtained for topographic profiles 1 to 24 ploted for (A) the roughness–length and (B) the compass methods of estimating fractal dimension

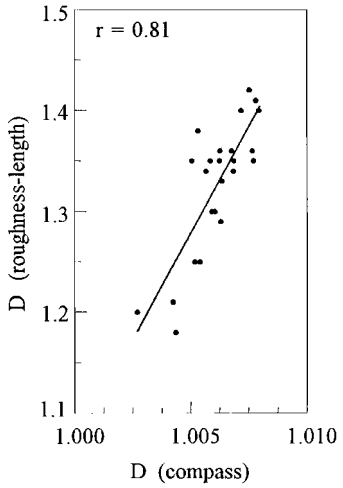

Figure 11. Cross-plot of compass and roughness–length dimensions computed for the Valley and Ridge topographic profiles

southwest, along strike. The fractal dimensions of structure and topography are compared in Figure 13 for both the roughness–length and compass measures. Regression lines fit to the fractal dimensions of structural relief and topographic relief yield correlation coefficients of 0·41 and 0·29, respectively (Figure 13). The slope of the regression line computed for the roughness–length dimensions is significantly positive at the $\alpha = 0{\cdot}025$ level, while that computed for the compass dimensions is significantly positive at $\alpha = 0{\cdot}1$. The variations in compass dimensions are more erratic than the roughness–length dimensions for both topography and structure.

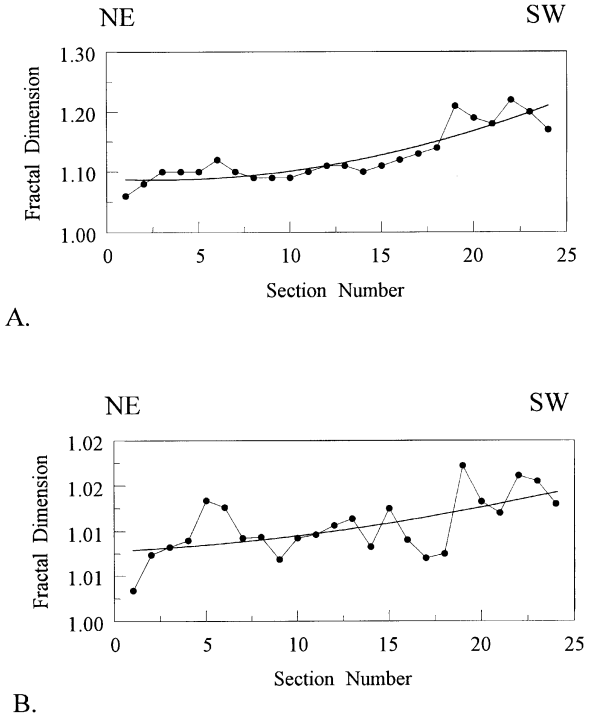

Figure 12. Fractal dimensions obtained for structural relief of the Onondaga Sandstone on profiles 1 to 24 plotted for (A) the roughness–length and (B) the compass methods of estimating fractal dimension

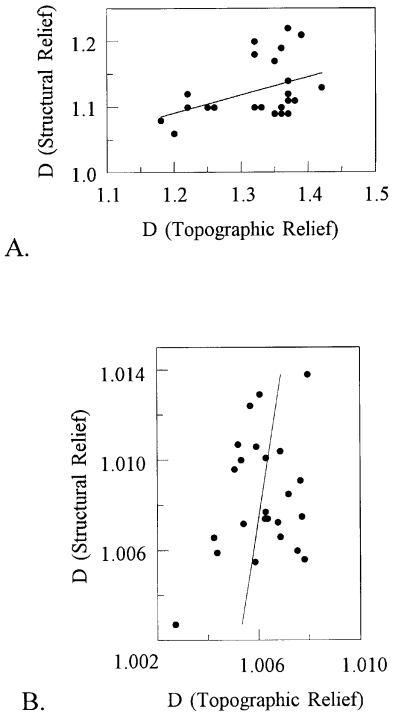

Figure 13. The fractal dimensions of topographic and structural relief cross-plotted for both (A) the roughness–length and (B) the compass estimation methods

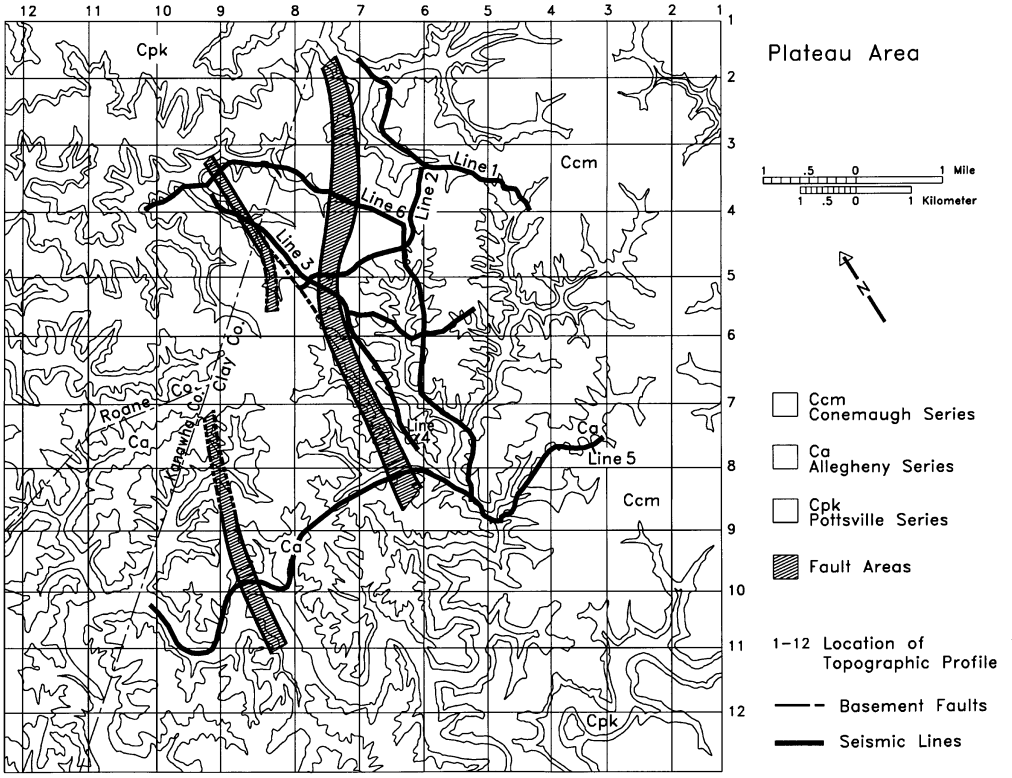

Figure 14. Geological map of the Appalachian Plateau study area. NE–SW and NW–SE topographic profiles 1–12 are located along with seismic lines across the area and major basement faults

The foregoing fractal analysis suggests not only that topographic relief is controlled in part by the relief of underlying structures, but also provides a quantitative assessment of the extent to which changes in the relative abundance and amplitude of different wavelength folds produce similar changes in the relative abundance and amplitude of different wavelength features in the surface topography. Fractals provide a quantitative assessment of the interrelationship between scale-dependent features in the topography and underlying structure.

APPALACHIAN PLATEAU

Surface geology across the Appalachian Plateau study area (Figures 2 and 14) consists of a relatively undeformed sequence of nearly flat-lying sandstones, limestones, shales and coals associated with Pennsylvanian (Carboniferous) age distributary channel deposits. Surface topographic patterns are reflected in the outcrop pattern formed by these flat-lying rock intervals Seismic Line 6 (Figure 15) crosses part of the study area (Figure 14) and reveals the presence of normal faults in the basement reflector at approximately 2 to 2·5 seconds two-way travel time. Conversion to depth of Line 6 (Figure 15) reveals that these basement faults have a combined offset of about 650 m. Structural relief across the near-surface Mississipian Greenbrier limestone reflector, however, does not exceed 50 m. The faults are associated with the east margin of the Rome Trough or Eastern Interior aulacogen (Harris, 1978). The seismic data reveal that the margin faults of this failed rift do not extend into the near-surface (Figures 15 and 16).

The fractal characteristics of the topography across this area were evaluated using 24 topographic profiles. Their locations form the grid lines in Figure 14. Elevations were digitized from USGS 7½ minute topographic quadrangles at approximately 15 m intervals. Twelve profiles were constructed along the northeast–southwest

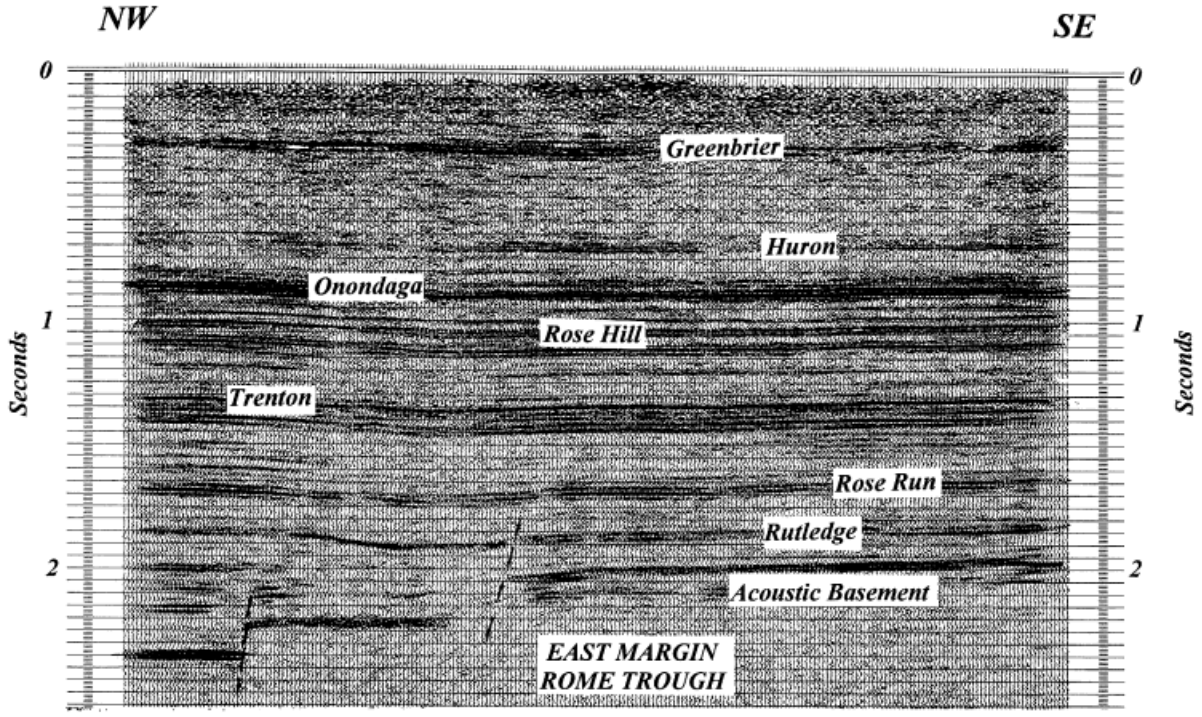

Figure 15. Seismic line from the Appalachian Plateau area (Line 6, Figure 18)

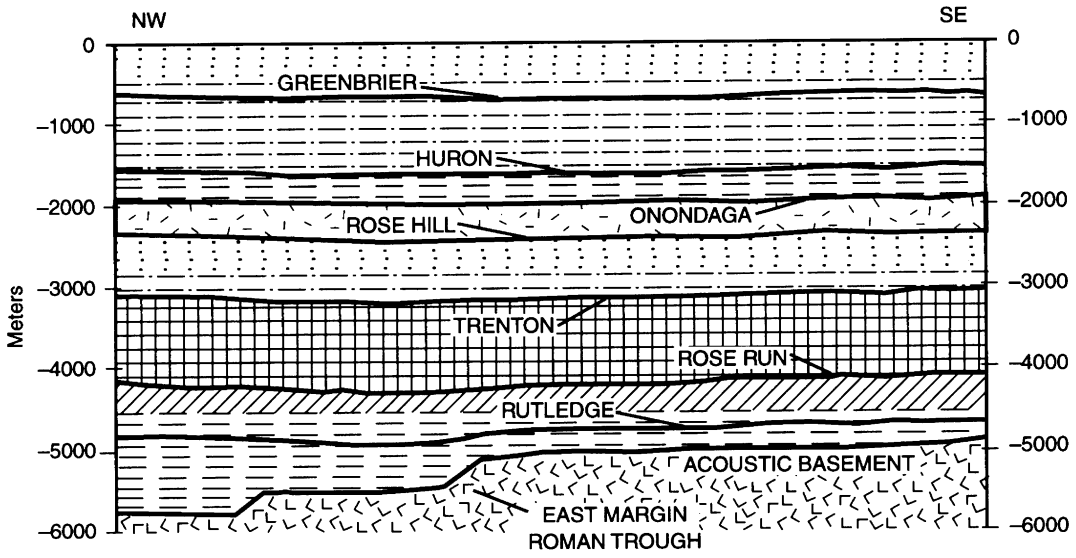

Figure 16. Depth section prepared from reflection event travel times observed on Line 6 and velocities from nearby sonic logs

subsurface structural trend and 12 profiles were constructed in the northwest-to-southeast dip direction (Figure 14). The dip profiles (Figure 17) reveal an almost random pattern of elevation variation, which is characteristic of the entire area. Fractal dimensions for the Plateau profiles were computed using only the roughness–length method. The Valley and Ridge study suggests that variations in the roughness–length dimensions are more

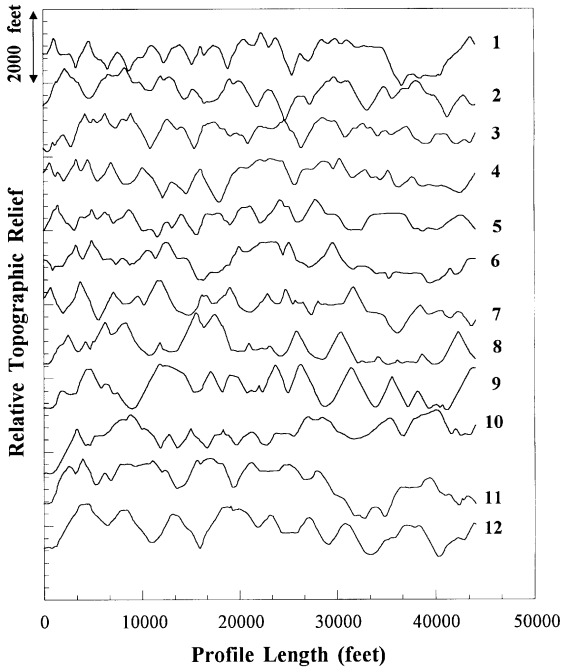

Figure 17. Topographic profiles crossing northwest-to-southeast across the Plateau study area

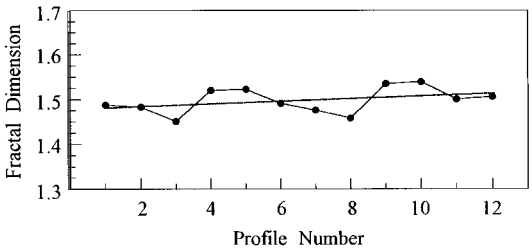

Figure 18. Fractal dimensions of the northeast–southwest oriented profiles through the Appalachian Plateau study area

consistent from profile to profile and provide a clearer representation of underlying trends than do the compass dimensions. Systematic variation of fractal dimension from one profile to the next does not appear in the dip profiles (Figure 18). The slope of the regression line fit to the fractal dimensions (Figure 18) is not significantly different from 0. The average value of fractal dimensions along the dip profiles (1·5) is not statistically different from those computed for the strike profiles (1·47). The average fractal dimension for the topography of the entire area (D=1·485) is significantly higher than that obtained for the Valley and Ridge profiles (D=1·33).

Fractal characteristics of the subsurface structure were analysed and compared to surface topography using a set of six vibroseis seismic lines from the area (Figure 14). The seismic data were available in digital form at a sample interval of 2 milliseconds. A computer picking algorithm was used to pick the reflection arrival times of the various events shown in Figure 15. Short wavelength trace-to-trace arrival time variations, most likely associated with noise, were removed or attenuated by filtering arrival time profiles with a low-pass Butterworth filter. A high cut wavenumber of 0·1 cycles per trace with 72 db per octave drop-off rate was used. The 0·1 wavenumber corresponds to a 10 trace (or sample) cycle in the data. The profiles are approximately 700 samples in length. Considerable short-wavelength variation remains in the data as illustrated in the shifted depth plot (Figure 19) constructed from the Line 6 interpretation (Figure 15). In the shifted depth display, reflector depth is shifted relative to the other events producing vertical exaggeration of profile relief and enhancement of subtle

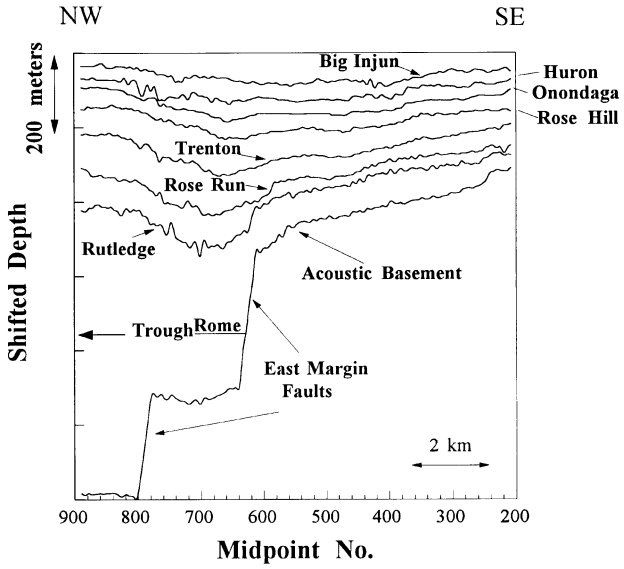

Figure 19. Shifted depth display enhances relative differences in relief. Events are plotted in sequential order without absolute depth reference

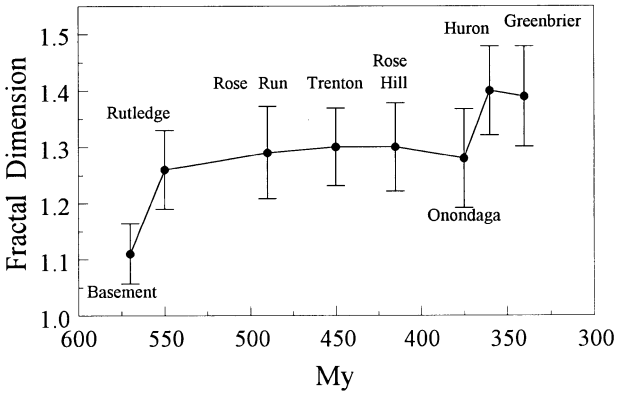

Figure 20. Mean fractal dimensions of reflection travel-time variations to the major reflection events observed on Lines 1 to 6 (Figure 14). Error bars represent the standard deviation of the sample mean for each event

structural features. The shifted depth format helps reveal the presence of short-wavelength features not apparent in either the seismic display (Figure 15) or depth section (Figure 16).

The fractal dimensions of interpreted reflection events were computed for all seismic lines. Average values of fractal dimension for each reflection event (Figure 20) reveal the presence of abrupt increases between the basement and Rutledge reflection events, and between the Onondaga and Huron events. Average fractal dimension was computed from six samples and chi-square tests reveal that the sample values are normally distributed. T-tests indicate that significant differences exist between the mean fractal dimensions of the basement and Rutledge reflection events and the Onondaga and Huron events at $\alpha = 0{\cdot}05$. Differences between the mean fractal dimensions of the Onondaga and Greenbrier events are less significant at $\alpha = 0{\cdot}1$. The variations in fractal dimension quantify differences in reflector geometry. The basement and Rutledge events span the Middle and Late Cambrian period of geological history. It was during this time that the main episode of failed rifting occurred (Shumaker and Wilson, 1996). The Onondaga and Huron events enclose a detachment interval in which a decollement is interpreted to have formed during the Allegheny orogeny.

Subsurface intervals coinciding with the Rutledge through Onondaga reflection events extend from the Late Cambrian to Lower Devonian periods. The fractal dimensions of reflectors in this interval average

approximately 1·29. Reactivation of basement faults in the area from Late Cambrian to lower Devonian time were relatively minor (Wilson *et al*., 1994). Another jump in fractal dimension occurs between the Lower Devonian Onondaga Limestone (D=1·28) and the Middle Devonian Huron Shale (D=1·4). Analysis of slickensides observed in cores from the Appalachian foreland (Evans, 1980, 1994) suggests that the Middle Devonian shales served as a detachment interval. Interpretation of the seismic data used in this study (Wilson *et al*., 1994; Hohn *et al*., 1994) reveal the presence of subtle detached structures above the Onondaga Limestone. The shallow Greenbrier and Huron reflection events have higher fractal dimension due to the presence of minor folds developed above a Middle Devonian decollement. Detached structures are concentrated in areas west of the trough margin.

The average fractal dimension of the shallow Greenbrier Limestone reflection event computed for portions of lines west of the margin (1·41) is slightly higher, but not statistically different from that for portions of the lines east of the margin (1·36). The absence of significant differences in the fractal characteristics of surface topography noted above is consistent with the lack of significant variation in near-surface structure. In general, the fractal dimensions of subsurface structure (inferred from travel-time data) increase towards the surface. This increase is associated with increased similarity in the amplitude of the different wavelength structural features. The different wavelength features in the Huron and Greenbrier reflection events have more similar amplitude compared to different wavelength features in the basement event. For the basement reflector, the longest-wavelength features are generated by normal faults and have much larger relief (amplitude) than the shorter-wavelength features present on individual fault blocks. This leads to the lower fractal dimension of the basement reflector. The average fractal dimension of the surface topography (1·49) is similar to that of the near-surface Greenbrier Limestone and follows the increases in fractal dimensions of subsurface structure from the basement to the near surface.

CONCLUSIONS

Topographic and structural relief examined in this study exhibit fractal behaviour as defined by roughness–length and compass estimates of fractal dimension. Studies conducted in intensely and mildly deformed tectonic environments of the North American Appalachian Mountains suggest that the presence or absence of variation in the fractal characteristics of surface topography are, in part, related to presence or absence of variations in the fractal characteristics of near-surface structure. The result is not surprising since subsurface structure distributes rocks of contrasting mechanical properties across the Earth's surface. The various processes of weathering and erosion then differentially etch topography into the Earth's surface according to the mechanical and chemical properties of the near-surface rock intervals. The use of fractals to compare topography and structure is preferred over regression line analysis since the fractal characteristics of a profile provide specific information about the abundance and relative amplitude of features in the profiles, whereas direct correlation of topographic and structural relief does not provide specific insight into properties that give rise to similarity.

Near-surface deformation in the Middle Mountain and Elkhorn Mountain area of the Valley and Ridge province is considerable. Changes in the fractal dimension of topographic relief are positively correlated to the fractal dimensions of near-surface structural relief. In the Appalachian Plateau area, significant near-surface deformation is absent and no change is observed in the fractal characteristics of topography across the area. Seismic data across the Plateau, however, reveal the presence of deeper subsurface structure associated with a Cambrian-age failed rift. Reactivation of rift structures was minimal to absent during and following deposition of near-surface intervals. Analysis of individual seisemic reflection events reveals that reflection arrival times and thus the subsurface structure are also fractal. Abrupt vertical changes in the fractal dimensions of reflection events are associated with stages in the evolution of the basin. The largest differences occur between syn- and post-rift sediments and across a decollement zone. The increase in fractal dimension observed across the decollement zone implies that intervals above the decollement are rougher or more highly deformed, as expected. Fractal analysis quantifies visually subtle differences in reflection arrival time variation and suggests the presence of varying structural complexity. In addition, fractal dimensions of subsurface intervals increase towards the near-surface where their fractal dimension is close in value to that of the surface topography.

This study suggests that topography cannot be simulated by a static fractal model. Fractal analysis reveals the presence of changes in complex topographic patterns over distances of only a kilometre or less that can be related to individual processes partially responsible for shaping the Earth's surface. Assessment of the fractal properties of topography might provide a useful remote sensing tool since systematic variations in complicated topographic patterns can be numerically represented by variations in their fractal dimension. In this study, variations in the fractal characteristics of topography are related to near-surface structural relief; however, where applicable, topographic change may be related to specific processes which themselves may be quantifiable as fractals (e.g. patterns of glaciation, fault trace patterns, reflectance, etc.) or to other numerical measures (e.g. shortening, fracture intensity, soil geochemistry, cumulative production, etc.).

ACKNOWLEDGEMENTS

The comments of anonymous reviewers were very helpful and significantly improved the manuscript. Drafting assistance provided by Debbie Benson and technical assistance provided by Joel Halverson were greatly appreciated. We thank Columbia Natural Resources in Charleston, WV, for providing some of the seismic data used in this project. Special thanks to Tom Mroz and Royal Watts of the Morgantown Energy Technology Center who supported this project through USDOE grant DE-FG21-95MC32158.

REFERENCES

Aki, K. 1981. 'A probabilistic synthesis of precursory phenomena', in Simpson, D. W. and Richards, P. G. (Eds), *Earthquake Prediction: An International Review*, Maurice Ewing Series, Vol. 4, 566–574.

Barton, C. D. and Hseih, P. A. 1989. 'Physical and hydrologic-flow properties of fractures', in American Geophysical Union, *28th International Geological Congress Field Trip Guidebook T385*, Washington, DC, 36 pp.

Evans, M. A. 1980. *Fractures in oriented Devonian shale cores from the Appalachian Basin*, MS thesis, West Virginia University, Morgantown, 278 pp.

Evans, M. A. 1994. 'Joints and decollement zones in Middle Devonian shales: Evidence for multiple deformation events in the central Appalachian Plateau', *Geological Society of America Bulletin*, **106**, 447–460.

Feder, J. 1988. Plenum Press. *Fractals*, 283 pp.

Gilbert, L. 1989. 'Are topographic data sets fractal?', *Pure and Applied Geophysics*, **131**, 241–254.

Goodchild, M. 1980. 'Fractals and the accuracy of geographical measures', *Mathematical Geology*, **12**(2), 85–98.

Hakenson, L. 1978. 'The length of closed geomorphic lines', *Mathematical Geology*, **10**, 141–167.

Harris, L. D. 1978. 'The Eastern Interior Aulacagen and its relation to Devonian shale gas production', in *Second Eastern Gas Shales Symposium*, USDOE Morgantown Energy Technology Center, DOE/METC/SP-78/6, **2**, 55–72.

Hirata, T. 1989. 'Fractal dimension of fault systems in Japan: Fractal structure in rock fracture geometry at various scales', *Journal of Pure and Applied Geophysics*, **131**(1/2), 157–170.

Hohn, E. H., Patchen, D. G., Heald, M., Aminian, K., Donaldson, A., Shumaker R. and Wilson, T. 1994. 'Measuring and predicting reservoir heterogeneity in complex deposystems: The fluvial deltaic Big Injun Sandstone in West Virginia', in *USDOE Final Report*, Contract No. DE-AC22-90BC14657, 116 pp.

Klinkenberg, B. and Goodchild, M. 1992. 'The fractal properties of topography: A comparison of methods', *Earth Surface Processes and Landforms*, **17**, 217–234.

Malinverno, A. 1990. 'A simple method to estimate the fractal dimension of self-affine series', *Geophysical Research Letters*, **17**(11), 1953–1956.

Mandelbrot, B. B. 1967. 'How long is the coast of Britain? Statistical self-similarity and fractional dimension', *Science*, **156**, 636–638.

Mandelbrot, B. B. 1977. *Fractals: Form, Chance and Dimension*, Freeman, San Francisco, 365 pp.

Mareschal, J. C. 1989. 'Fractal reconstruction of sea-floor topography', *Journal of Pure and Applied Geophysics*, **131**(1/2), 197–210.

Mark, D. and Aronson, P. 1984. 'Scale-dependent fractal dimensions of topographic surfaces: An empirical investigation, with applications in geomorphology and computer mapping', *Mathematical Geology*, **16**(7).

Rundle, J. B. 1989. 'Derivation of the complete Gutenberg-Richter magnitude-frequency relation using the principle of scale invariance', *Journal of Geophysical Research*, **94**(89), 12 337–12 342.

Shumaker, R. C. and Wilson, T. H. 1996. *Basement structure of the Appalachian foreland in West Virginia. Its style and affect on sedimentation*, Geological Society of America Special Paper.

Turcotte, D. L. 1986. 'A fractal model for crustal deformation', *Tectonophysics*, **132**, 261–269.

Turcotte, D. L. 1989. 'Fractals in geology and geophysics', *Pure and Applied Geophysics*, 171–196.

Turcotte, D. L. 1992. *Fractals and Chaos in Geology and Geophysics*, Cambridge University Press, 221 pp.

Walsh, J. J. and Watterson, J. 1993. 'Fractal analysis of fracture patterns using the standard box-counting technique: valid and invalid methodologies', *Journal of Structural Geology*, **15**(12), 1509–1512.

Wilson, T. H. 1997. 'Fractal strain distribution and its implications on cross-section balancing: further discussion', *Journal of Structural Geology*, **19**(1), 129–132.

Wilson, T. H. and Shumaker, R. C. 1988. 'Three-dimensional structural interrelationships within the Cambrian–Ordovician lithotectonic unit of the Central Appalachians', *Bulletin of the American Association of Petroleum Geologists*, **72**(5), 600–614.

Wilson, T. H. and Shumaker, R. C. 1992. 'Broad top thrust sheet: An extensive blind thrust in the central Appalachians', *Bulletin of the American Association of Petroleum Geologists*, **76**(9), 1310–1324.
Wilson, T., Shumaker, R. and Zheng, L. 1994. 'Sequential development of structural heterogeneity and its relationship to oil production: Granny Creek, West Virginia', in Schultz, A. and Rader, E. (Eds), *Studies in Eastern Energy and the Environment*, Mineral Resources Special Publication **132**, 20–25.
Wilson, T. H., Dominic, J. and Halverson, J. 1996. 'Fractal interrelationships in field and seismic data', in *US Department of Energy Final Report*, Grant No. DE-FG21-95MC32158.
Wu, S. 1993. 'Fractal strain distribution and its implications on cross-section balancing', *Journal of Structural Geology*, **15**, 1497–1507.

